Supplementary Materials

Size-dependent electrobending in piezoceramics mediated by gradient defect dipoles

Haoyu Gu[1], Zehua Deng[2], Siqing He[1], Hu Zhao[1], Shaoqi Huang[1], Shuwen Zhang[1], Linlan Li[1], Shubao Shao[1,*] and Minglong Xu[1,**]

1. State Key Laboratory for Strength and Vibration of Mechanical Structure, School of Aerospace Engineering, Xi'an Jiaotong University, Xi'an, 710049, China
2. Shanghai Institute of Satellite Engineering, Shanghai 200240, China

* Corresponding author. Email: ssb_xjtu@xjtu.edu.cn
** Corresponding author. Email: mlxu@xjtu.edu.cn

Formula derivation section

Determination of parameters in general solution

Based on Kirchhoff's thin plate theory, the governing equation for the circular thin plate is given by

$$D\nabla^4 w(r) = q(r), \#(S1)$$

where $D = \frac{Et^3}{12(1-\nu^2)}$ represents the bending stiffness, ν is Poisson's ratio, $w(r)$ denotes the deflection, and $q(r)$ is the applied force. Since the circular thin plate is solely subjected to a bending moment, i.e. $q(r) = 0$, Eq. S1 can be expressed as

$$\frac{d}{dr}(r\frac{d}{dr}(\frac{1}{r}\frac{d}{dr}(r\frac{dw}{dr}))) = 0. \#(S2)$$

The general solution to Eq. S2 is given by

$$w(r) = C_1 r^2 lnr + C_2 r^2 + C_3 lnr + C_4, \#(S3)$$

here C_1, C_2, C_3, and C_4 are pending parameters that can be determined by boundary conditions.

Since the deflection is finite at the center of the disk, $C_3 = 0$, otherwise the function $w(r)$ diverges at $r = 0$. The bending moment $M(r)$ is also finite at $r = 0$, and

$$M(r) = -D\left(\frac{d^2w}{dr^2} + \frac{\nu dw}{r\,dr}\right) = -D\left[2C_1(1+\nu)lnr + (3+\nu)C_1 + 2C_2(1+\nu)\right]. \#(S4)$$

Therefore, $C_1 = 0$, otherwise $M(r)$ also diverges at $r = 0$. Furthermore, at $r = R$, $w(R) = 0$ and $M(R) = M$, i.e.

$$\begin{cases} C_2R^2 + C_4 = 0 \\ -2D(1+\nu)C_2 = M \end{cases}. \#(S5)$$

Based on the above boundary conditions, the pending parameters can be determined as follows:

$$\begin{cases} C_1 = C_3 = 0 \\ C_2 = -\frac{M}{2D(1+\nu)}. \#(S6) \\ C_4 = \frac{MR^2}{2D(1+\nu)} \end{cases}$$

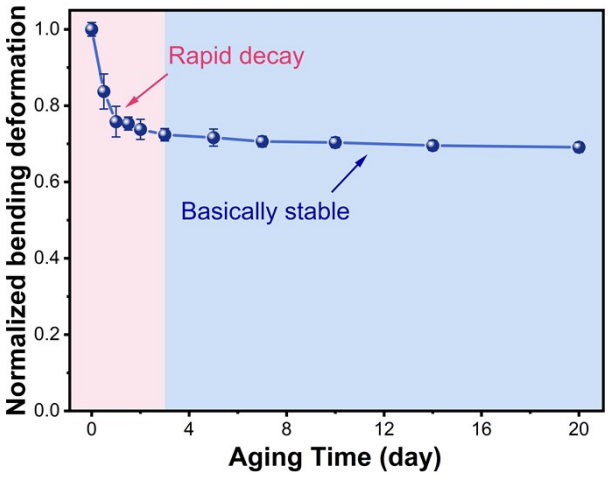

Fig. S1. The relationship between normalized bending deformation and aging time.

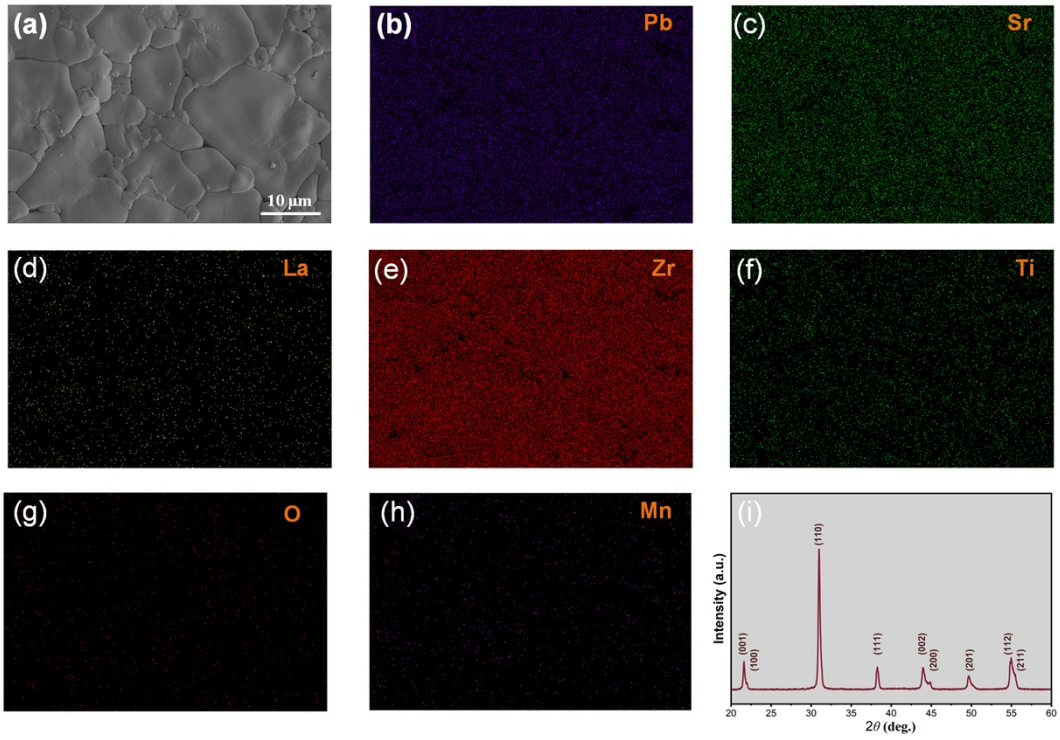

Fig. S2. Structure characterization of PSLZT-0.10Mn ceramics. (a) SEM images of the ceramic surface. (b-h) The in-situ energy-dispersive spectrum (EDS) mapping of Pb, Sr, La, Zr, Ti, O and Mn, respectively. (i) XRD patterns of PSLZT-0.10Mn ceramic.

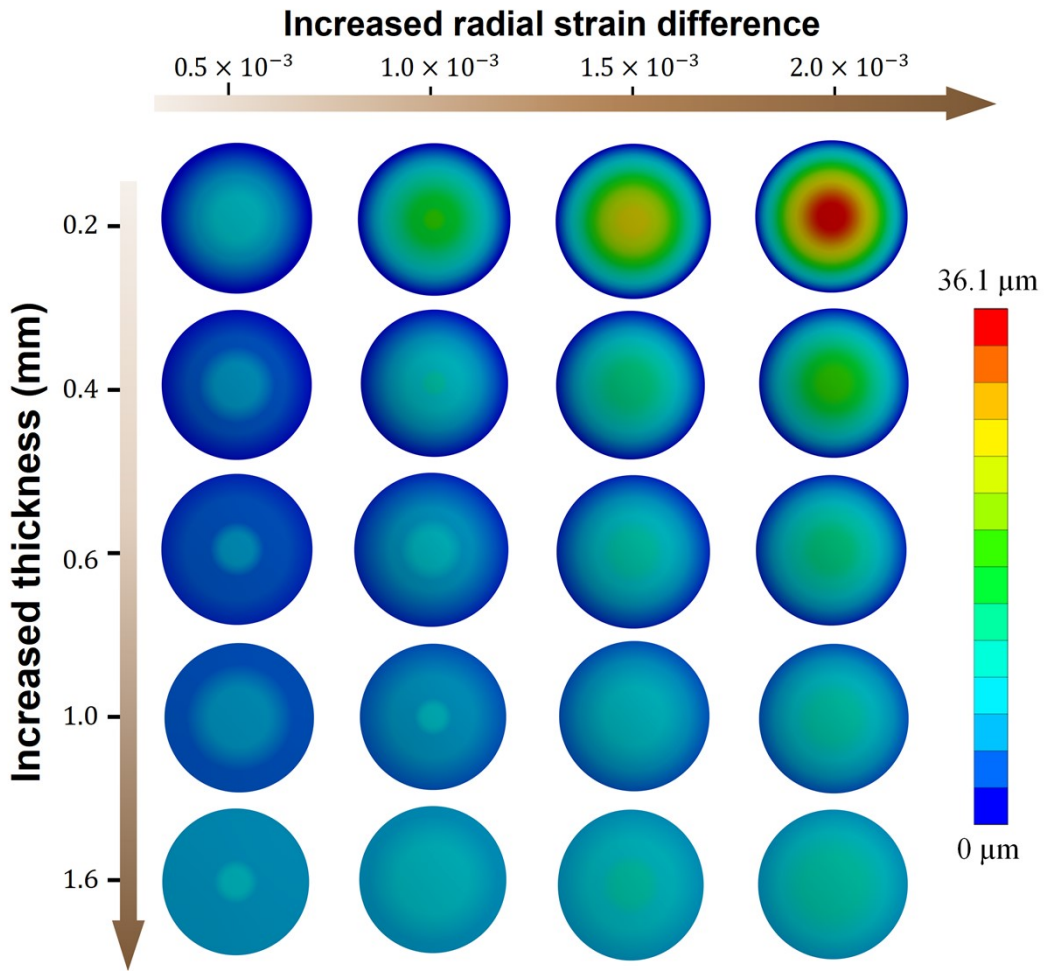

Fig. S3. FEM results of samples with various radial strain difference and thickness, with a radius of 10 mm.

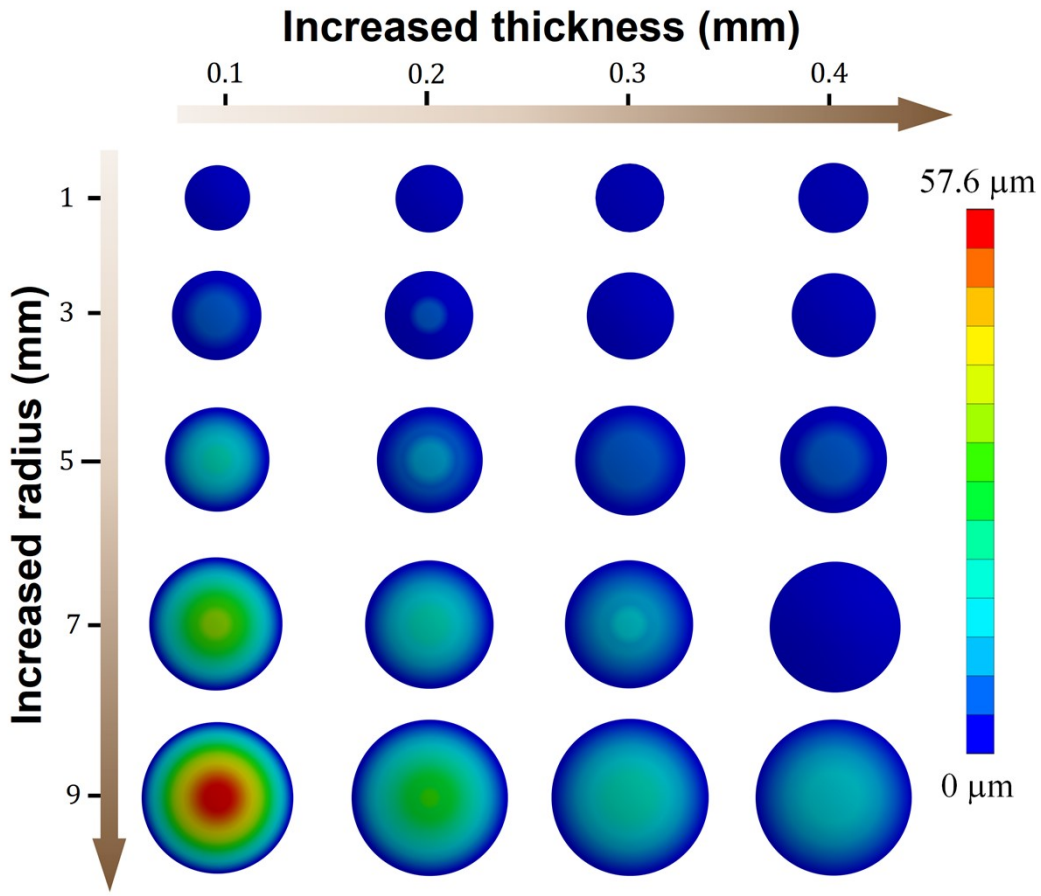

Fig. S4. FEM results of samples with various thickness and radius, with a radial strain difference of 2.0×10^{-3}.

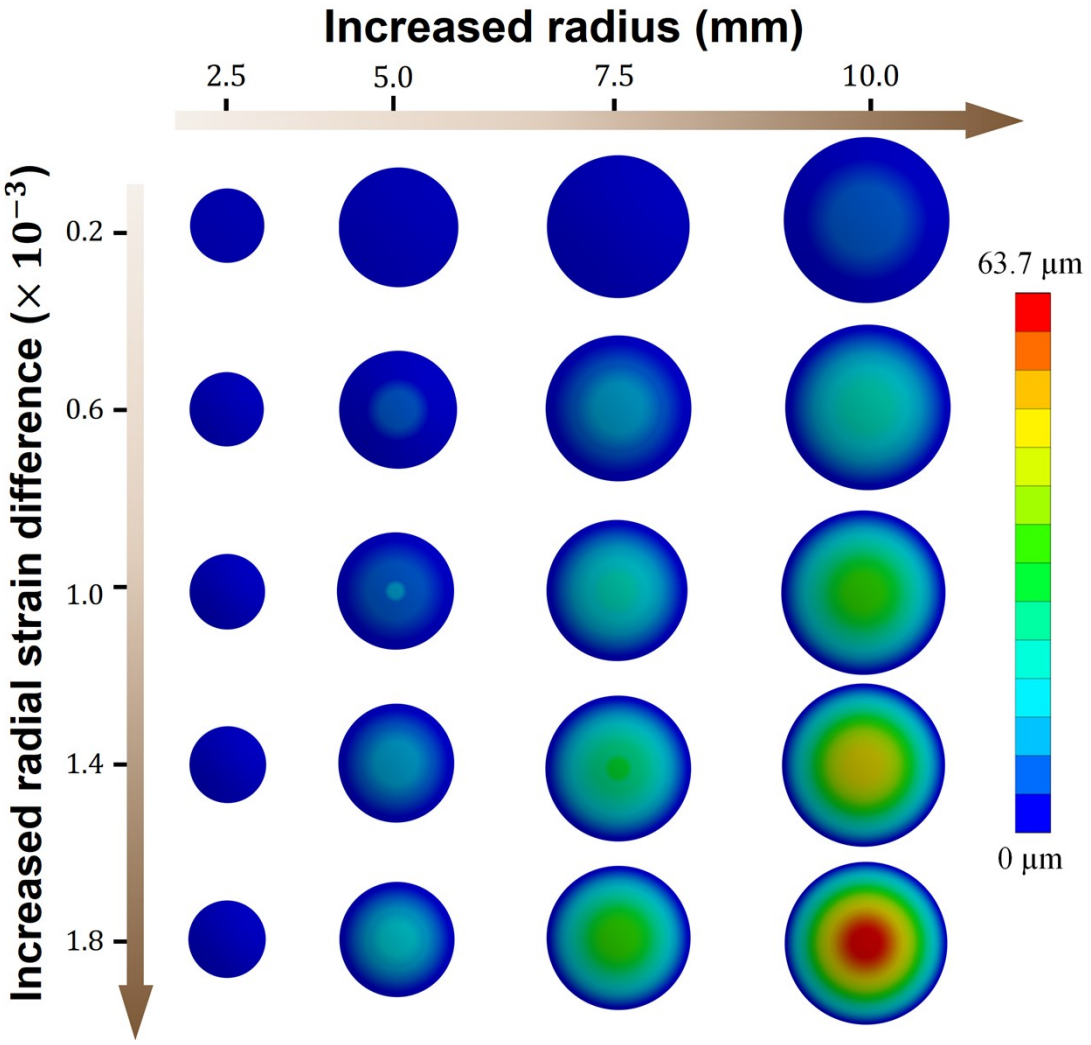

Fig. S5. FEM results of samples with various radial strain difference and radius, with a thickness of 0.1 mm.

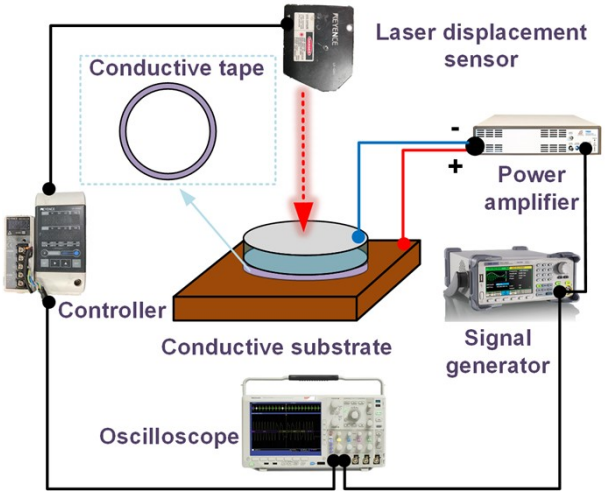

Fig. S6. Schematic diagram of the custom-built displacement measurement system.

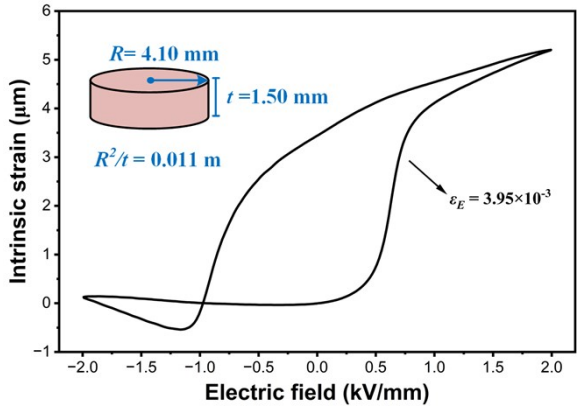

Fig. S7. Intrinsic *S*-*E* curve of PSLZT-0.10Mn piezoceramic under an electric field of ±2 kV/mm.

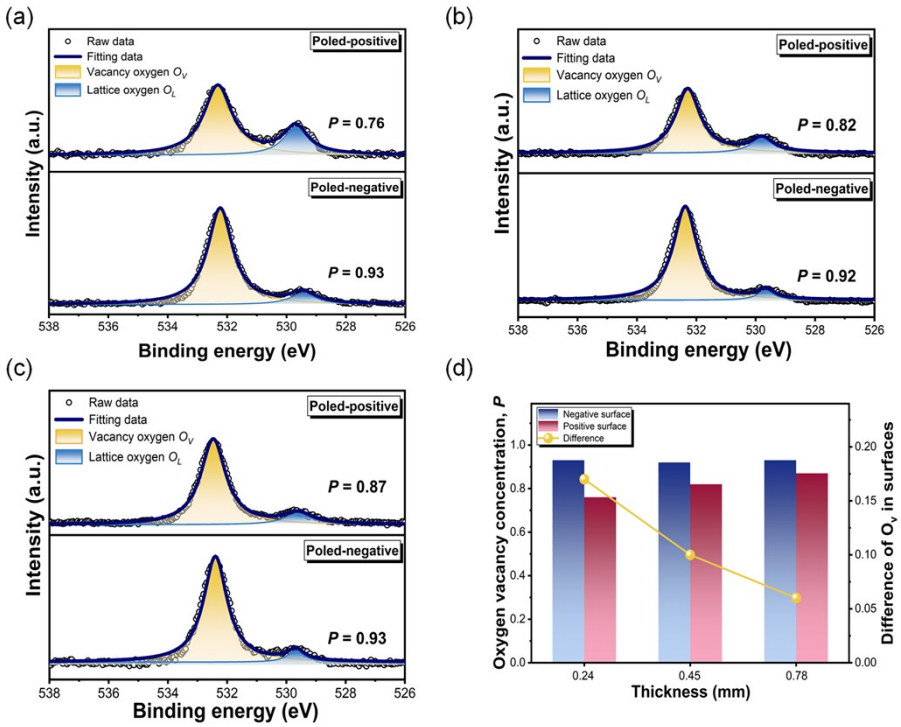

Fig. S8. The thickness dependence of oxygen vacancy concentration distribution. XPS of the O1 s orbitals for positive and negative surface of samples with (a) t = 0.24 mm, (b) t = 0.45 mm, and (c) t = 0.78 mm. (d) The concentration and difference of oxygen vacancies on the positive and negative surfaces vary with the thickness.